Chapter 5

Chemical Pressure effect at the boundary of Mott insulator and itinerant electron limit of Spinel Vanadates

5.1 Introduction

Mott insulators are important examples of strongly correlated materials. The strong-coupling limit, $U >> t$ (U is the inter-atomic Coulomb energy and t is the spin dependent expectation value for the charge transfer between sites), corresponds to materials in which valence electrons are strongly localized in their atomic orbitals (Mott-Hubbard insulator). The opposite weak-coupling limit, $U << t$, corresponds to correlated metals whose electrons are completely delocalized (Paramagnetic metal). This implies that a Mott transition is induced at a critical value Uc/t [1]. As a matter of fact, paramagnetic metals and Mott-Hubbard insulators represent two fundamentally different phases that can be interchanged by increasing or decreasing electronic correlations through a first-order quantum phase transition (QPT) [2]. It is highly challenging to characterize the electronic properties of materials when approaching the QPT either from Mott insulator side or from the paramagnetic metal side. Among very few materials, the AV_2O_4 spinels are a family of Mott insulators that fulfil the criterion of varying the t/U ratio because of the metal-metal separation can be changed by applying the chemical pressure i.e., by changing the size of the A^{2+} cation [3]. The absence of e_g electrons makes direct V-V hybridization between t_{2g} orbitals the only relevant contribution to the hopping amplitude. Moreover, t is also a function of the interionic distance, R. This volume dependence between d orbitals is $J/V^{-10/3}$ [4], which is the basis of the phenomenological Bloch's equation [5] for magnetic insulators: $\alpha = \partial \ln T_N / \partial \ln V = -3.3$ provided U remains constant. When approached towards itinerant-electron behaviour the α value is very sensitive so that it can indicate the applicability of crystal-field theory [6, 7].

ZnV$_2$O$_4$ has one of the smallest charge gaps among the vanadium spinels: ($\Delta \approx$ 0.55 eV) [8, 9]. Therefore, with proper doping on A-site this ZnV$_2$O$_4$ may be transferred to the Mott transition. In a recent report [10] a clear evidence of pressure dependence of a non-monotonic behaviour of charge gap was shown. The non-monotonic dependence of charge gap on t/U is expected for materials that are deep inside the Mott regime (small t/U ratio) [11,12] and the enhancement of the magnetic up-up-down-down ordering along the [±1,0,1] and [0,±1,1] chains has already been reported in these vanadates [13].

ZnV$_2$O$_4$ crystallizes in a cubic spinel structure, where the V atoms form a pyrochlore lattice of corner-sharing tetrahedra. As a matter of fact, the antiferromagnetic

(AF) interactions between the V atoms are highly frustrated. At T_S = 51 K, ZnV_2O_4 undergoes a structural phase transition where the symmetry is lowered from cubic to tetragonal (c/a < 1) with a compression of the VO_6 octahedron along the c axis [14] and the system possibly orbital orders. This also lifts the geometrical frustration of the cubic phase making way for the second transition at T_N = 40 K which is of a magnetic nature and the system orders antiferromagnetically [14-16]. The lattice formed by the V atoms can be described as built up by V-V chains running along the [110], [011], and [101] directions. The magnetic structure, found by neutron diffraction [13,14], is AF along the [110] direction (within the ab plane), but along the [101] and [011] (off plane) directions the V moments order. Moreover, the effective hopping and the d-d transfer integral of ZnV_2O_4 estimated from the X-ray photoemission spectra are close to the metallic LiV_2O_4 [17].

Moreover, it has been shown that in ZnV_2O_4 away from the strong-coupling regime bond and magnetic ordering are independent to each other [10]. If the bond ordering is strengthened away from the strong-coupling regime then it may correspond to ferroelectricity as is observed in CdV_2O_4 [18]. It has also been suggested by Kuntscher et al. [10] that ferroelectricity can be increased significantly by decreasing V-V distance as the structural distortion observed in ZnV_2O_4 is identical to CdV_2O_4. Furthermore, the main limiting factors for ZnV_2O_4 to show spontaneous polarization are the losses or leak currents. The increase in the value of charge gap reduces the losses. In ZnV_2O_4 when external pressure is applied, which lead to the decrease in V-V distance, the charge gap increases above a critical pressure [10]. As the V-V separation decreases the system moves towards the itinerant electron limit [3]. Therefore, closing the Mott gap of this geometrically frustrated Mott insulator is a potential route for enhancing ferroelectricity which could be achieved in ZnV_2O_4 by reducing the V-V distance. Chemical substitution is the best way to doing this.

In the present paper we have varied the chemical pressure in ZnV_2O_4 by doping Mn and Co on the Zn site and studied the effect of it on magnetic, optical, transport properties and on electron structure of doped and undoped ZnV_2O_4. We have also doped Ti on the V site and varied the metal-metal distance and observed its effect. Our results support the universality of the first order character of the transition from the localized to the itinerant-electron and the stabilization of an intermediate phase in which there is a

disproportionation into molecular orbitals within clusters and weak bonding between clusters [19, 20].
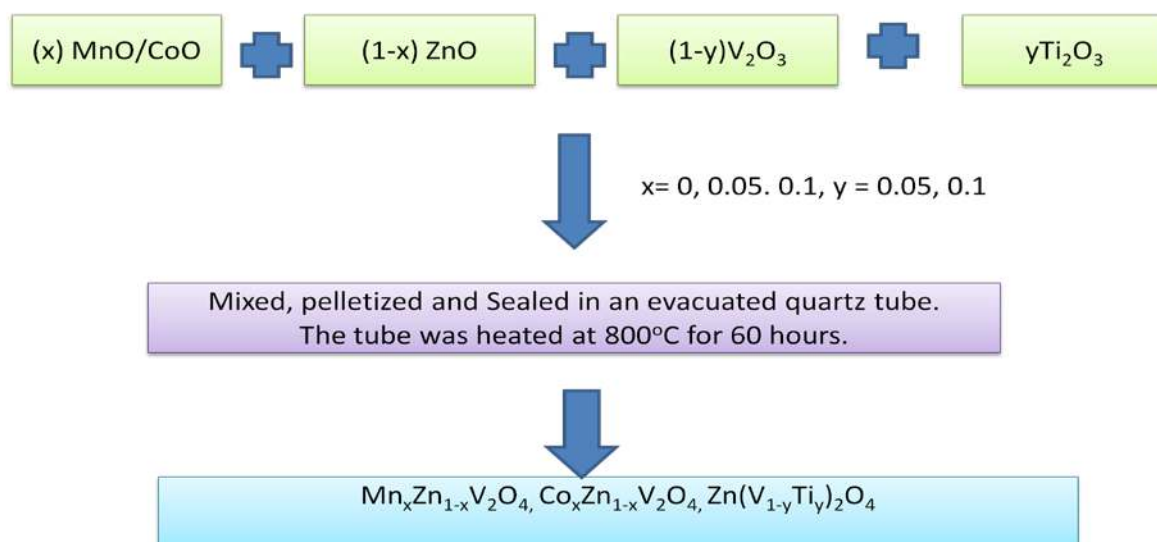
5.2 Experimental

Fig. 5.1. *Block diagram of solid state reaction technique to synthesize $Mn_xZn_{1-x}V_2O_4$, $Co_xZn_{1-x}V_2O_4$ and $Zn(V_{1-y}Ti_y)_2O_4$.*

Polycrystalline $(Zn_{1-x}Mn_x)V_2O_4$, $Zn_{0.9}Co_{0.1}V_2O_4$ and $Zn(V_{1-x}Ti_x)_2O_4$ (where x = 0, 0.05 and 0.10) were prepared by solid state reaction route. Appropriate ratio of ZnO, CoO, V_2O_3, Ti_2O_3 and MnO were mixed and pressed into pellets. The pellets were sealed in quartz tube under high vacuum and heat treated into furnace at 800 ^{o}C for 60 hrs. The X-ray diffraction measurement was performed at 10 K and at room temperature. The magnetic measurements were done with Vibrating Sample magnetometer (VSM). Fourier transform infrared spectroscopy measurements have been done using Spectrum 65 FTIR spectrometer (Perkin Elmer Instruments, USA) in the range of 500 to 4000 cm^{-1}. Resistivity measurements has been performed by four probe method and thermoelectric power measurement (Seebeck coefficient) has been done using home-made thermoelectric setup. X-ray Photoelectron Spectroscopy (XPS) experiments were performed using Omicron Nanotechnology UHV system equipped with a twin anode Mg/Al X-ray source (DAR400), a monochromator and a hemispherical electron energy analyzer (EA125 HR). All the XPS measurements were

performed inside the analysis chamber under base vacuum of 5.0×10^{-10} Torr using monochromatized AlKα. The total energy resolution, estimated from the width of the Fermi energy, was about 300 meV for monochromatic AlKα line with photon energy 1486.60 eV.
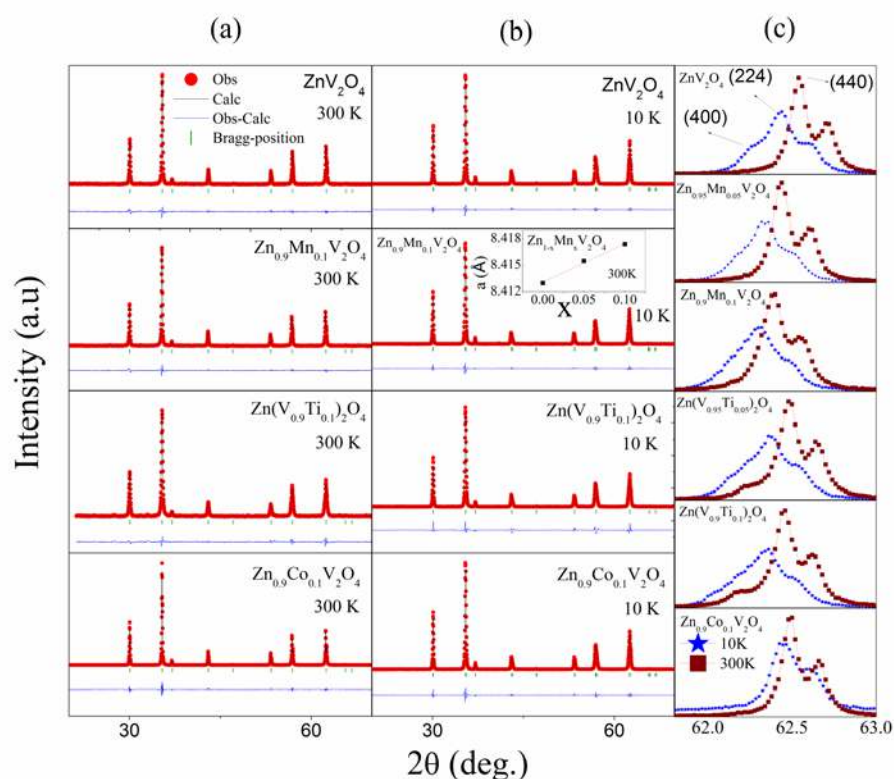
5.3 Results and Discussion

Fig. 5.2. *X-ray diffraction pattern with Reitveld refinement for Mn, Co and Ti doped ZnV₂O₄ samples at (a) 300 K and (b) 10 K. (c) X-ray diffraction pattern in very narrow 2θ (61.5°-63°) range at 300K (above the structural transition) and at 10 K. Inset shown the variation of Manganese concentration with lattice parameter.*

The XRD measurement of all the samples indicates the single phase nature of the samples. The samples crystallize in cubic phases with Fd-3m space group. At low temperature (structural transition temperature) the structure changes to tetragonal phase with I41/a space group. We have refined the diffraction data using the Fullprof program [shown in Fig.5.2 (a) and (b)] and the fitted parameters are shown in Table 5.1. The X-ray diffraction pattern of Mn and Ti doped samples have been shown (Fig. 5.2 (c)) in a very narrow 2θ (61.5°–63°) range at 300 K (above the structural transition) and at 10 K (below the structural transition, if any). A very weak splitting is observed for 10% Mn and Co

doped samples in the 10 K diffraction pattern indicating the decrease of structural distortion. Moreover, for Ti doped samples also structural transition is reduced. The estimated c/a ratio for undoped sample is 0.9892, whereas, for 10% Mn, Co and Ti doped samples it is ~0.9894, ~0.9897 and ~0.9893 respectively.

Table 5.1 *Structural parameters (lattice parameters, bond lengths) of $Zn_{1-x}A_xV_2O_4$ (with x=0, 0.05, 0.1 and A=Mn, Co, Ti) samples obtained from Reitveld refinement. The structural data have been refined with space group I41/a at10 K and Fd-3m at 300 K.*

ZnV_2O_4	10 K	a (Å)	5.9481(1)	d(Zn-O)(Å)	4 × 1.96874(4)
		b (Å)	5.9481(1)	d(V-O) (Å)	2×2.00193(7), 4×2.02377(3)
		c (Å)	8.3713(4)	d(V-V)(Å)	2×2.96689(6), 4×2.97406(7)
	300 K	a (Å)	8.4130(1)	d(Zn-O)(Å)	4×1.974774 (3)
				d(V-O) (Å)	6×2.01864(3)
				d(V-V)(Å)	6×2.97446(3)
$Zn_{0.95}Mn_{0.05}V_2O_4$	10 K	a (Å)	5.9503(3)	d(Zn-O)(Å)	4×1.970(6)
		b (Å)	5.9503(3)	d(V-O) (Å)	2×2.003(7), 4×2.024(4)
		c (Å)	8.3769(2)	d(V-V)(Å)	2×2.97517(8), 4×2.96843(6)
	300 K	a (Å)	8.4155 (2)	d(Zn-O)(Å)	4×1.975359(3)
				d(V-O) (Å)	6×2.01924(2)
				d(V-V)(Å)	6×2.97534(2)
$Zn_{0.9}Mn_{0.1}V_2O_4$	10 K	a (Å)	5.9540(4)	d(Zn-O)(Å)	4×1.97083(8)
		b (Å)	5.9540(4)	d(V-O) (Å)	2×2.00432(12), 4×2.02578(7)
		c (Å)	8.3813(1)	d(V-V)(Å)	2×2.97700(15), 4×2.97013(10)
	300 K	a (Å)	8.4174 (1)	d(Zn-O)(Å)	4×1.97579(2)
				d(V-O) (Å)	6×2.01968(4)
				d(V-V)(Å)	6×2.97599(5)
$Zn(V_{0.95}Ti_{0.05})_2O_4$	10 K	a (Å)	5.9487(2)	d(Zn-O)(Å)	4×1.96893(5)
		b (Å)	5.9487(2)	d(V-O) (Å)	2×2.00210(10), 4×2.02398(5)
		c (Å)	8.3719(7)	d(V-V)(Å)	2×2.97436(10), 4×2.96716(8)
	300 K	a (Å)	8.4115 (6)	d(Zn-O)(Å)	4×1.97442(3)
				d(V-O) (Å)	6×2.01828(5)
				d(V-V)(Å)	6×2.97393(5)
$Zn(V_{0.9}Ti_{0.1})_2O_4$	10 K	a (Å)	5.9487(2)	d(Zn-O)(Å)	4×1.96898(8)
		b (Å)	5.9487(2)	d(V-O) (Å)	2×2.00227(12), 4×2.02398(7)
		c (Å)	8.3726(8)	d(V-V)(Å)	2×2.96728(10), 4×2.97435(15)
	300 K	a (Å)	8.4102 (7)	d(Zn-O)(Å)	4×1.97411(3)
				d(V-O) (Å)	6×2.01796(5)
				d(V-V)(Å)	6×2.97345(5)
$Zn_{0.9}Co_{0.1}V_2O_4$	10 K	a (Å)	5.9466(2)	d(Zn-O)(Å)	4×1.96860(4)
		b (Å)	5.9466(2)	d(V-O) (Å)	2×2.00248(7), 4×2.02327(4)
		c (Å)	8.3736(1)	d(V-V)(Å)	2×2.97331(8), 4×2.96692(6)
	300 K	a (Å)	8.4111(9)	d(Zn-O)(Å)	4×1.97431(2)
				d(V-O) (Å)	6×2.01817(4)
				d(V-V)(Å)	6×2.97377(4)

Moreover, The lattice parameter "a" for the Mn doped samples obtained from the Reitveld refinement of the room temperature XRD data is shown as a function Mn content in the inset of Fig. 5.2(b). From the figure, it is clear that with increase of Mn content the lattice parameter increases, which is due to lower ionic size of Zn^{2+}(0.74 Å) compared to Mn^{2+} (0.80 Å). The linear dependence of the lattice constant on Mn concentration indicates that there is no structural change in ZnV_2O_4 with Mn doping and as a matter of fact Zn is replaced by Mn into the crystal lattice following the Vegard's law [21]. In the similar way Co and Ti also replace respectively to Zn and V.

In order to support the crystallinity in the investigated samples we have also shown the transmission electron micrographs (TEM) of all the samples in Fig. 5.3. TEM image shows the clear crystallinity with cubic phase.
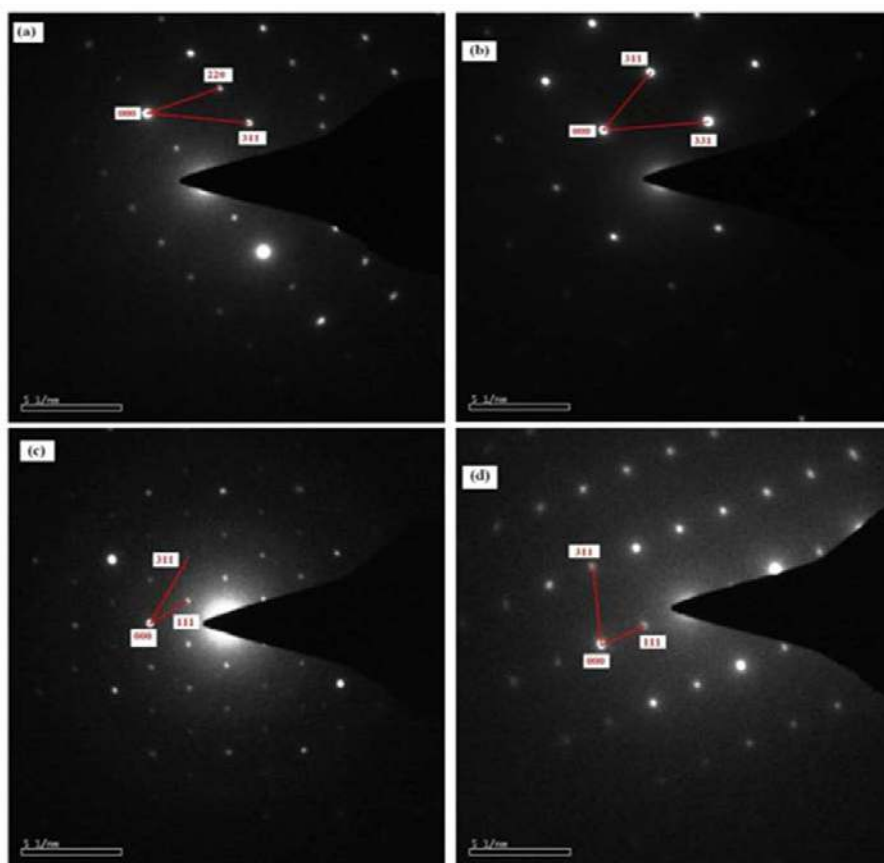

Fig. 5.3. *TEM images of (a) ZnV_2O_4, (b) $Zn_{0.9}Mn_{0.1}V_2O_4$, (c)$ZnV_{1.8}Ti_{0.2}O_4$, (d) $Zn_{0.9}Co_{0.1}V_2O_4$.*
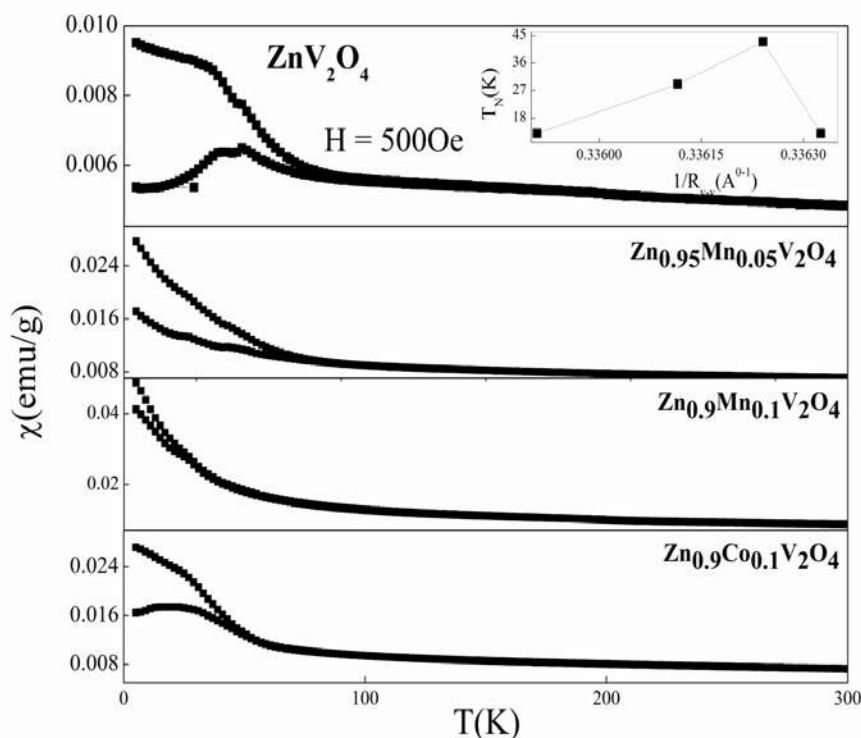
Fig. 5.4. *Temperature variation of magnetization for $Zn_{1-x}A_xV_2O_4$ [where x=0.05 and 0.1 for A=Mn and x =0.01 for A = Co] spinels at H=500 Oe. Inset: Variation of T_N with the inverse V-V distance, $1/R_{V-V}$ for the $Zn_{1-x}A_xV_2O_4$ [where x=0.05 and 0.1 for A=Mn and x =0.01 for A = Co] spinels.*

Magnetization curves of $Zn_{1-x}A_xV_2O_4$ [A=Mn and Co] measured for different doping concentration are shown in Fig. 5.4. For ZnV_2O_4 two clear transitions are observed where the higher temperature is the structural transition and the lower temperature is the magnetic transition [14-16]. It is observed that with increase of doping concentration the peak appears due to structural transition is reduced which is consistent with the XRD measurement. In the inset of figure 5.4 the evolution of T_N with the V-V separation for the $Zn_{1-x}A_xV_2O_4$ [A=Mn and Co] spinels has been shown. It is to be mentioned that as the overlap integral in t of $J \propto t^2/U$ [J is the super exchange spin-spin interaction] increases with decreasing R_{V-V}, the energy U must decrease or remain constant. As a matter of fact, within the localized-electron superexchange, T_N should increase with decreasing V-V separation. In the present investigation it has been observed when Mn is doped the V-V separation increases and subsequently T_N decreases. On the other hand, when Co is doped it is observed that V-V separation decreases very slightly, but interestingly T_N decreases. This suggests that the energy U in the localized electron superexchange theory is not

when Co is doped. Recently it has been shown [22] in $Mn_{1-x}Co_xV_2O_4$ system that as Co content increases T_c also increases. It has also been shown that with increase of Co doping the V-V separation decreases. Therefore, the reported system is within the localized-electron superexchange limit which is consistent with our present Mn doped sample. But the behaviour of the present Co doped samples are consistent with the $Cd_{1-x}Zn_xV_2O_4$ system [23]. It has been explained that the disorder nature of Cd and Zn affect the V site orbital ordering which in effect reduces the T_N. Therefore, in the present case the site-disorder might also be a probable reason of decrement of T_N with Co doping. But for the present Co-doped ZnV_2O_4 system no spin glass like behaviour is observed which is expected for the site-disorderness.
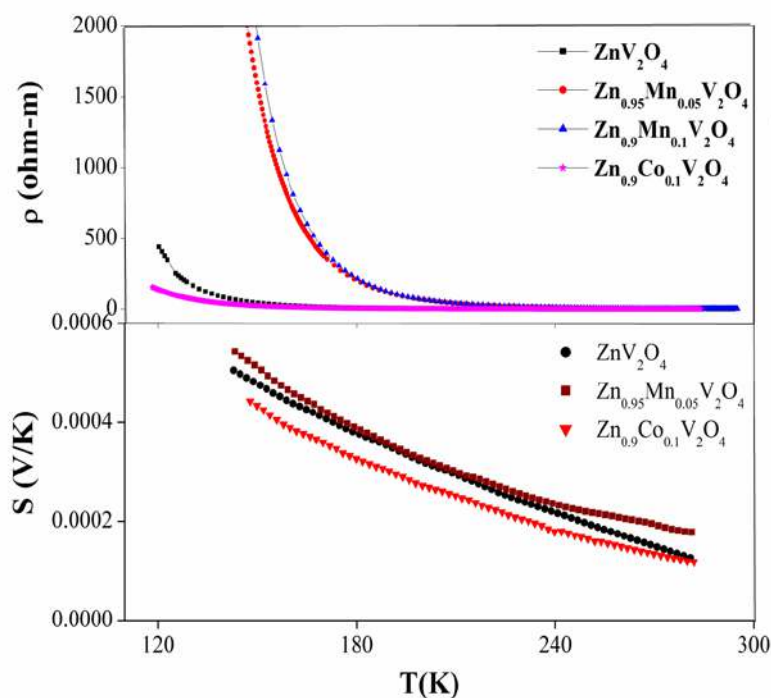

Fig. 5.5. *Upper panel: Temperature dependent Resistivity curves for Mn and Co doped ZnV_2O_4. Lower panel: Temperature dependent of thermoelectric power for $Zn_{1-x}A_xV_2O_4$ [where x=0.05 for A=Mn and x =0.10 for A = Co].*

As mentioned above, the variation of T_N with V-V distance can be interpreted as the consequence of a variation of U/t, which collapses close to the itinerant limit. According to this, even though ZnV_2O_4 and Co-doped ZnV_2O_4 are still semiconducting, a partial electronic delocalization along the V-V bonds may occur as has been anticipated by Pardo

110

et al. [8] for their ZnV_2O_4 and MgV_2O_4 samples which are at the boundary between itinerant and localization limits. In Fig. 5.5 we have shown the experimental resistivity curves for Mn and Co doped and undoped ZnV_2O_4 in which the V-V distances are different. The results show the activation energy decreases with the decrease of V-V distance as the metal-insulator transition is approached from the localized-electron side confirming the reduction of U/t with decrease of V-V distance, which might be due to a partial delocalization of electrons [3] and in this limit neither the localization-electron model and nor the itinerant-electron model is applicable as has been mentioned by Blanco-canosa *et al.* [3]. It is observed from the resistivity curve at low temperature with the decrease of V-V distances the V^{3+}-3d electrons approaches to the Quantum Phase Transition (QPT) from the localized-electron side. It is worthwhile to mention here that CoV_2O_4 itself has the lower activation energy and lower resistivity indicating that the CoV_2O_4 approaches the itinerant limit [24]. In the lower panel of Fig. 5.5 the temperature dependence of the thermoelectric power, S(T) is shown for all the spinels mentioned above. The S(T) value is large and positive which indicates that there is only a low density of mobile holes in these vanadates. Thermally activated behaviour of small polarons for all these vanadates is observed. Therefore, the possibility of the existence of the large polaron which forms due to non-stoichiometry can be excluded. Also, the S value decreases from Mn-doped to undoped to the Co-doped ZnV_2O_4 sample.

Moreover, it is observed that ZnV_2O_4 and Co doped ZnV_2O_4 exhibit low activation energy compared to the Mn doped ZnV_2O_4 samples. In consistent with the earlier study [3] a structural transition from the low temperature tetragonal to a high temperature cubic phase is observed. These transitions are due to a co-operative ordering of strong V-V bonding as is observed from XRD refinement. It is found for Mn doped samples the V-V bonding becomes weaker and it moves towards the localized electron side. As is already mentioned that the estimated phenomenological parameter is unfeasible in the Mn-doped samples, therefore, U>>t might be the case in this Mn doped samples which are in localized electron side.
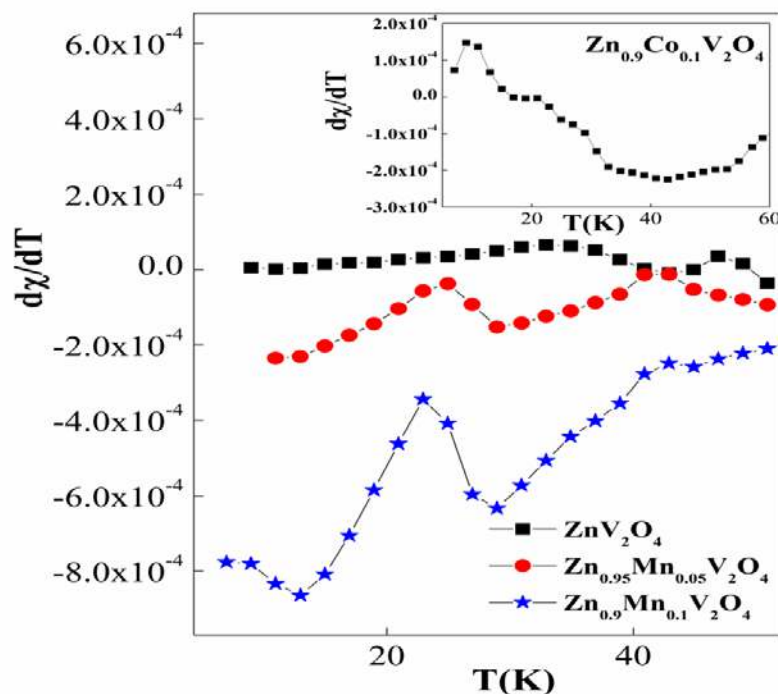
Fig. 5.6. *dχ/dT as a function of Temperature for Mn and Co doped ZnV₂O₄.*

Furthermore, it is observed in Fig. 5.4 the susceptibility drops sharply for ZnV_2O_4 and Co-doped ZnV_2O_4 on cooling through the structural transition temperature. This is due to the spin-pairing of V-V bonds [3]. For Mn doped samples this kind of sharp drop is not observed. Furthermore, from the $d\chi/dT$ vs T plot (Fig. 5.6) it is observed that with increase of Mn content the high temperature peak which is associated with the structural transition is diminished. This behaviour i.e. the suppression of the orbital ordering when it is going towards the Mott-regime (t<<U) is consistent with those already reported [11,12].

We have also measured the transmittance of all the samples and plotted the absorbance as a function of frequency in Fig. 5.7. A peak is observed below 1000 cm^{-1} which is due to one of the four phonon modes as is observed for cubic spinels. The absorbance spectra show a strong onset above 1000 cm^{-1}. The variation of charge gap (Δ), estimated from the intersection of the linear extrapolation of the absorption edge and the frequency axis, with the inverse of V-V distance is shown in Fig. 5.8. The Δ initially decreases with increase of V-V distance and with further increase of V-V distance it increases sharply. This non-monotonous behaviour is consistent with that of the external pressure effect [10]. This

result we have confirmed by plotting the activation energy (estimated from the resistivity measurement) as a function of inverse V-V distance [Fig. 5.9].
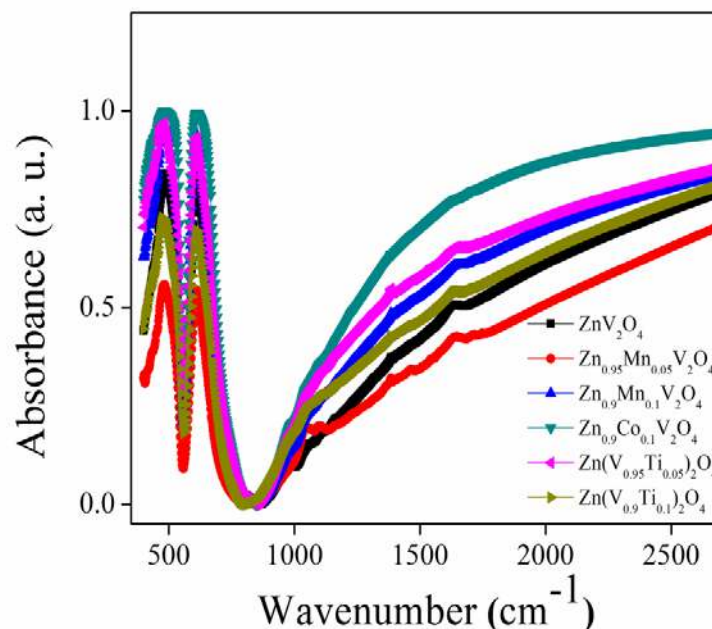

Fig. 5.7. *Room temperature Absorbance Spectra of $Zn_{1-x}A_xV_2O_4$ [where x=0.05 and 0.1 for A=Mn and x =0.1 for A = Co] and $Zn(V_{1-x}Ti_x)_2O_4$ [where x=0.05 and 0.1].*
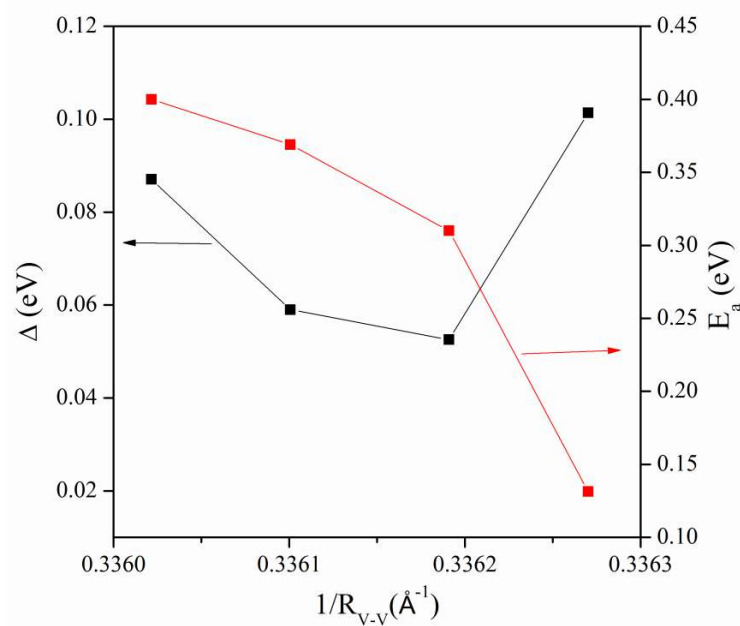

Fig. 5.8. *Charge gap and activation energy variation as a function of inverse V-V distance for $Zn_{1-x}A_xV_2O_4$ [where x=0.05 and 0.1 for A=Mn and x =0.01 for A = Co].*
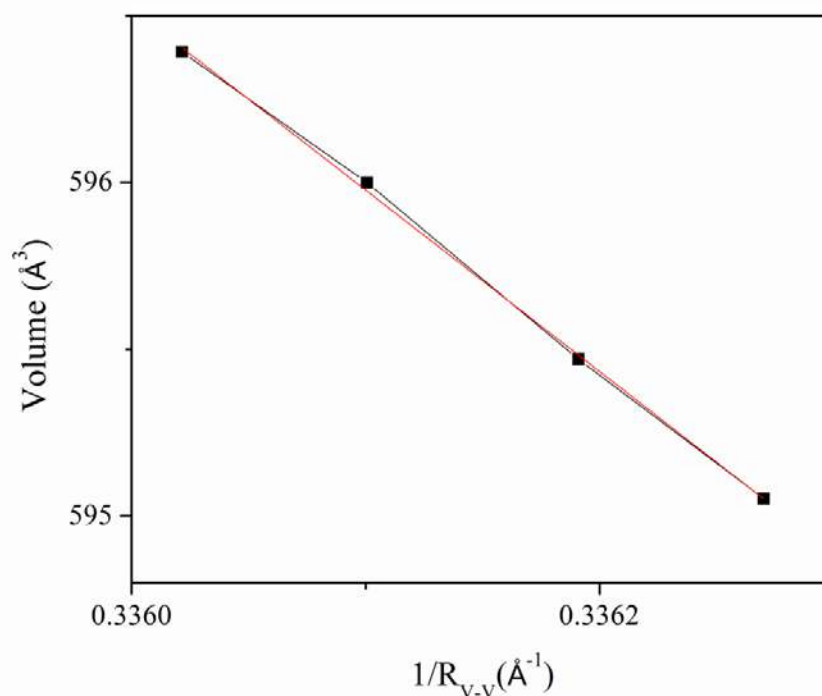
Fig. 5.9. *Variation of Volume as a function of $1/R_{V-V}$ for $Zn_{1-x}A_xV_2O_4$ [where x=0.05 and 0.1 for A=Mn and x =0.01 for A = Co].*

We have seen that the variation of activation energy with chemical pressure is consistent with that of charge gap variation with chemical pressure. It has already been proposed [8] that in ZnV_2O_4 the V-V dimmers form along the [011] and [101] directions together with an up-up-down-down magnetic order along the same directions. Moreover, in chemical pressure dependence of sample volume [Fig. 5.9] an anomaly is observed for the V-V distance 2.9736 Å. This is consistent with the inverse V-V distance variation of charge gap data. It might be the fact that stabilization of dimerized phase occurs below the V-V distance 2.9736 Å. Similar kind of behaviour is observed when 10-12 GPa pressure is applied on ZnV_2O_4 system. Therefore, it might be predicted that 10-12 GPa pressure reduces the V-V distance to 2.9736Å. Therefore, we see from the above discussion that T_N, charge gap and activation energy of different spinel vanadates depends on the V-V separation and as it decreases a breakdown of localized electron model for the 3d electrons is observed. This observation is consistent with those observed previously [3,10]. The shortest V-V distance we have obtained in Co doped ZnV_2O_4 and that distance is 2.9738 Å

which is larger than the critical distance for electron itinerancy (2.84 Å) [20]. This is similar to the case of $MgTi_2O_4$ where a tetramerization of the Ti chains is observed [25].
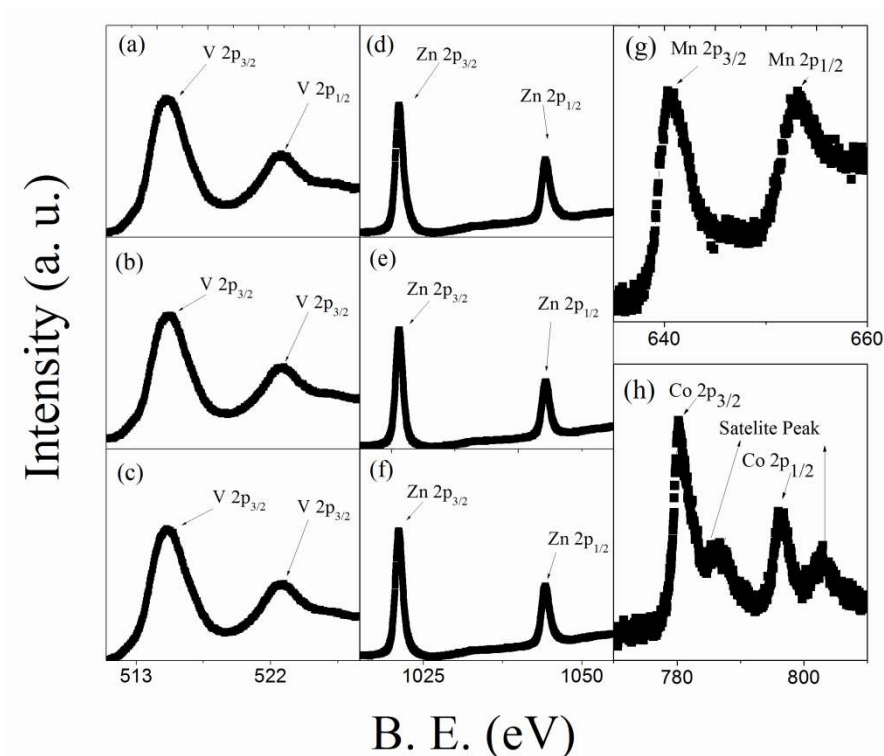

Fig. 5.10. *V 2p XPS core-level spectra of ZnV_2O_4 (a), $Zn_{0.9}Mn_{0.1}V_2O_4$ (b) and $Zn_{0.9}Co_{0.1}V_2O_4$ (C); Zn 2p XPS core-level spectra of ZnV_2O_4 (d), $Zn_{0.9}Mn_{0.1}V_2O_4$ (e) and $Zn_{0.9}Co_{0.1}V_2O_4$ (f); Mn 2p XPS core-level spectra of $Zn_{0.9}Mn_{0.1}V_2O_4$ (g); Co 2p XPS core-level spectra of $Zn_{0.9}Co_{0.1}V_2O_4$ (h).*

We have also studied the electronic structure of Mn and Co doped ZnV_2O_4 using x-ray photoemission spectroscopy (XPS). The purpose of this study is to see what happens in the electronic structures when the system is moving from itinerant electron side to localized electron side and vice versa and to provide clues to understand the origin of charge and orbital orderings in the spinel-type V oxides with tetragonal distortions. The XPS core-level spectra of Zn 2p, V 2p, Mn 2p and Co 2p of ZnV_2O_4, Mn and Co doped ZnV_2O_4 are shown in Fig. 5.10. All the core level spectra show $2p^{3/2}$ and V $2p^{1/2}$ states. Both Mn 2p and Co 2p spectra show satellites peaks. The two clear distinct states of V $2p^{3/2}$ and V $2p^{1/2}$ observed at ~7.6 eV apart, due to spin-orbit splitting. The V $2p^{3/2}$ spectrum of ZnV_2O_4 indicates a V^{3+} single valence level and no indication of the existence of V^{4+} (or V^{5+})

component as has been observed in some other reports [26-28]. All the core level spectra show $2p^{3/2}$ and V $2p^{1/2}$ states. Both Mn $2p$ and Co $2p$ spectra show satellites peaks. The two clear distinct states of V $2p^{3/2}$ and V $2p^{1/2}$ observed at ~7.6 eV apart, due to spin-orbit splitting. The V $2p^{3/2}$ spectrum of ZnV_2O_4 indicates a V^{3+} single valence level and no indication of the existence of V^{4+} (or V^{5+}) component as has been observed in some other reports [26-28].
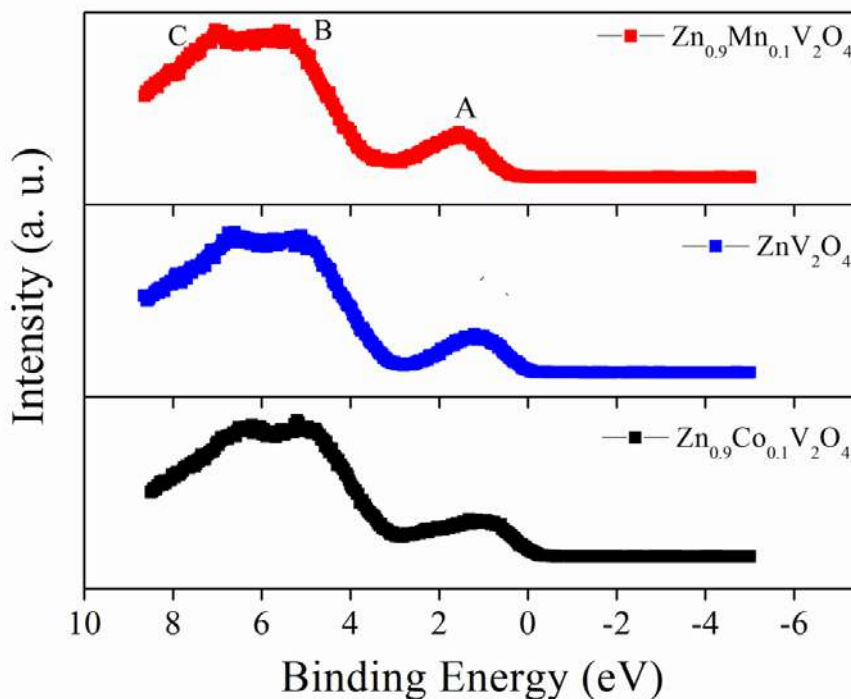

Fig. 5.11. *Valance-band XPS spectra of ZnV_2O_4, $Zn_{0.9}Mn_{0.1}V_2O_4$ and $Zn_{0.9}Co_{0.1}V_2O_4$.*

Three features (A, B and C) are observed in the valence-band spectra for ZnV_2O_4, and Mn and Co doped ZnV_2O_4 (Fig. 5.11). Feature (A) close to Fermi level (E_F) can be assigned to the antibonding band of the V $3d$ t_{2g} states hybridized with the O $2p$ states, while features B and C are due to the bonding band of the O $2p$ states hybridized with the V $3d$ t_{2g} and e_g states, respectively [29-30]. The position of A shifts to the E_F in going from Mn doped ZnV_2O_4 to ZnV_2O_4 to Co doped ZnV_2O_4 and, consequently, the magnitude of the band gap in t_{2g} bands decreases in this order. The magnitude of the band gap for ZnV_2O_4 ~0.2 eV which is in good agreement with that estimated from the resistivity data. In the case of Co doped ZnV_2O_4, the V $3d$ band reaches very close to E_F, consistent with the resistivity behavior. The binding energy of feature B for Co doped ZnV_2O_4 (4.79 eV),

corresponding to the *p-d* charge transfer energy, is small compared to those for ZnV_2O_4 and Mn doped ZnV_2O_4 (~5.32 eV).

Takubo *et al.* [17] calculated the tight-binding (TB) parameters for ZnV_2O_4 and CdV_2O_4 using Harrison's rule [31] where the parameters were defined as $(pd\sigma)\alpha 1/(R_{V\,O})^{3.5}$.

Table 5.2. *Tight-binding parameters for ZnV_2O_4, $Zn_{0.9}Mn_{0.1}V_2O_4$ and $Zn_{0.9}Co_{0.1}V_2O_4$.*

Sample		Distance(Å)						
	Phase	V-V	V-O	$dd\sigma$	$pd\pi$	Δ(ev)	T_σ	T_π
ZnV_2O_4	Cubic	2.97446	2.01864	-0.4639	0.9321	4.89	-0.3479	-0.1778
	Tetragonal	2.96689, 2.97406	2.02377, 2.00193	-0.4742, -0.4685	0.9305, 0.9666		-0.3557, -0.3514	-0.1771, -0.1911
$Zn_{0.9}Mn_{0.1}V_2O_4$	Cubic	2.97599	2.01968	-0.4627	0.9304	5.32	-0.3470	-0.1627
	Tetragonal	2.97013, 2.97700	2.02578, 2.00432	-0.4716, -0.4662	0.9237, 0.9625		-0.3537, -0.3497	-0.1604, -0.1741
$Zn_{0.9}Co_{0.1}V_2O_4$	Cubic	2.97377	2.01817	-0.4645	0.9329	4.79	-0.3484	-0.1817
	Tetragonal	2.96692, 2.97331	2.02327, 2.00248	-0.4741, -0.4691	0.9313, 0.9656		-0.3556, -0.3518	-0.1811, -0.1947

$(dd\sigma)\alpha 1/(R_{V\text{-}V})^5$, $(pd\sigma)/(pd\pi)=(dd\sigma)/(dd\pi)=-2.16$ and $R_{V\text{-}O}$ and $R_{V\text{-}V}$ are the bond lengths between the neighboring V and O sites and between the neighboring two V sites, respectively. The set for the structural parameters and TB parameters are listed in Table 5.2. The *pdπ* value for Co doped ZnV_2O_4 (~0.95 eV) is slightly larger than that for ZnV_2O_4 (0.94eV) and Mn doped ZnV_2O_4 (0.93eV). Also it is observed that the *ddσ* value increases slightly in going from Co doped ZnV_2O_4 (−0.52 eV) to ZnV_2O_4 (−0.47 eV) to Mn doped

ZnV_2O_4 (−0.40 eV). As a result, the effective hopping due to *d-d* transfer $T\sigma=3/4(dd\sigma)$ is ranging from −0.350 eV to −0.356 eV, while the effective hopping due to *p-d* transfer $T\pi=-(pd\pi)^2/\Delta$ is ranging from −0.185 eV to −0.21 eV. Here, the values of Δ are estimated from the XPS spectra. This indicates that the exchange interaction due to *d-d* transfer is dominant in the systems. The magnitude of T_σ gradually decreases in going from Co doped ZnV_2O_4 to ZnV_2O_4 to Mn doped ZnV_2O_4. The above results show that variations of different parameters with doping are not so significant. But the tendency clearly indicates that Co-doped ZnV_2O_4 are closer to the itinerant electron limit. Takubo et al. [17] has also shown that for metallic LiV_2O_4 the *pdπ value is larger but ddσ* value is smaller compared to the semiconducting ZnV_2O_4 and CdV_2O_4. This also supports our observation.

Takubo et al. [17] have explained the XPS for ZnV_2O_4 and CdV_2O_4 by orbital-driven Pierls (ODP) and complex linear combination orbitals (COO) model [32, 33]. The ODP scenario is based on the assumptions that the t_{2g} band has one-dimensional character due to the dominant *d-d* direct hopping and that the t_{2g} band has itinerant character due to the closeness to the metal-insulator transition. The present photoemission study shows the large *ddσ* values indicating the the dominant *d-d* direct hopping and this increases from Mn doped ZnV_2O_4 to Co doped ZnV_2O_4 through ZnV_2O_4. Moreover from the above discussion on valence band spectra it is observed that V 3d band reaches closer to the E_F from Mn doped to Co doped ZnV_2O_4 through ZnV_2O_4. Therefore, when it is going towards the smaller R_{V-V} the Pierls Physics is becoming important over Mott Physics.
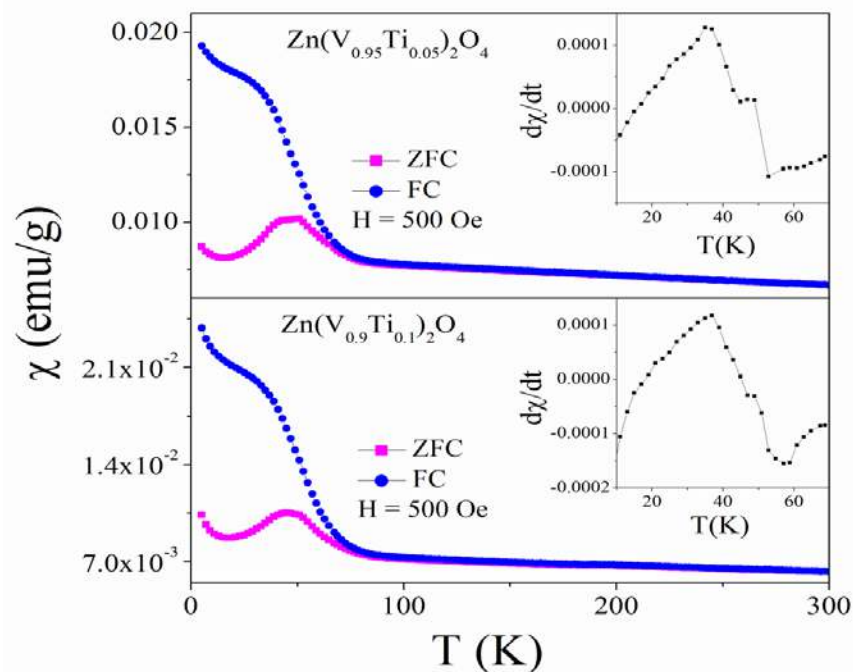
Fig. 5.12.*Valance Temperature variation of magnetization measured at H=500 Oe for Zn(V$_{1-x}$Ti$_x$)$_2$O$_4$ [where x=0.05 and 0.1].*

In the present investigation we have also doped Ti on the Vanadium site of ZnV$_2$O$_4$ to vary the metal-metal distance. It is observed from the refinement of the XRD data that with increase of Ti content the metal-metal distance increases. On the other hand, with
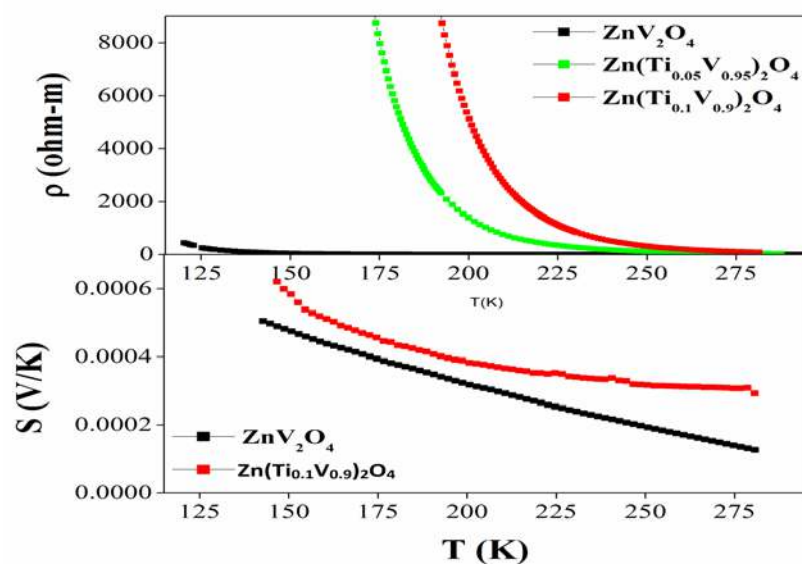

Fig. 5.13. *Temperature dependent Resistivity and Seeback Coefficient for Zn(V$_{1-x}$Ti$_x$)$_2$O$_4$ [where x=0.05 and 0.1].*

increase of Ti content the T_N, charge gap and the activation energy also increase [Figs.5.12, 5.13 and 5.14]. As is already mentioned with localization electron model with increase of metal-metal distance the T_N should decrease. But in the present case as Ti is doped opposite behaviour is observed. It may happen that Ti-doping decreases the intra-atomic Coulomb energy U which in effect increases the T_N. Nevertheless, it deserves further study to explain these interesting phenomena.
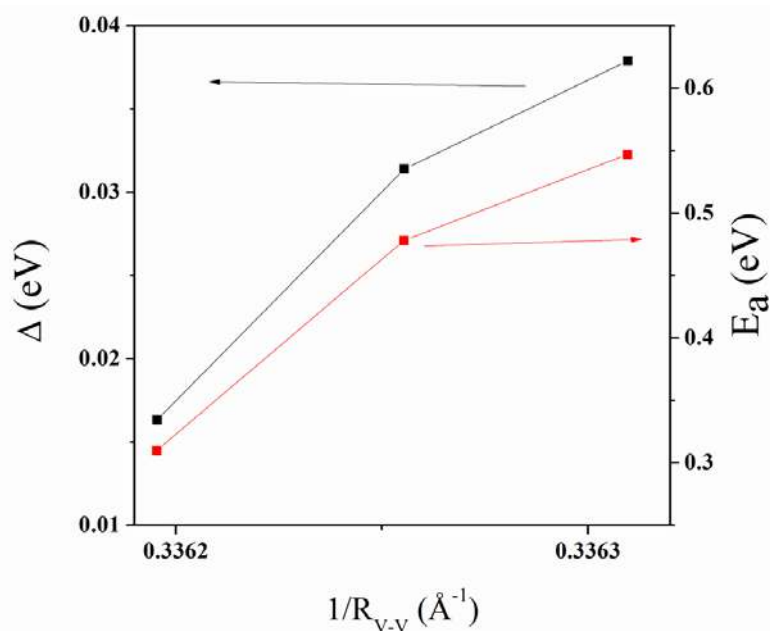

Fig. 5.14. *Variation of Charge gap and Activation energy as a function of $1/R_{V-V}$ for $Zn(V_{1-x}Ti_x)_2O_4$ [where x=0.05 and 0.1].*

Moreover, $MgTi_2O_4$ undergoes a M-I transition on cooling below $T_{MI} \sim 260$ K, accompanied by a strong decrease of the magnetic susceptibility and a transition to a tetragonal structure [34]. The structure in this composition was found to contain dimmers with short Ti-Ti distances (2.85 Å), the locations of the spin singlets. The electronic structure is consistent with the opening of a 1 eV gap and the absence of magnetic moments and enables one to interpret the crystal structure in terms of orbital ordering [20]. But in the present case when Ti is doped the metal-metal distances increase. That might be reason of interesting behaviour observed in this Ti doped samples.

5.4 Conclusion

The magnetization behavior indicates that when 10% Mn and Co are doped in ZnV_2O_4 the intensity of peak which arises due to the structural transition decreases. When Mn is doped the resistivity and thermoelectric power increase along with the increase of V-V distance. When Co is doped the V-V separation decreases very slightly, but T_N decreases which suggests that the inter-atomic Coulomb energy U in the localized electron superexchange theory is not constant when Co is doped. The activation energy decreases with the decrease of V-V distance as the metal-insulator transition is approached from the localized-electron side which confirms the reduction of U/t with decrease of V-V distance, which might be due to a partial delocalization of electrons and in this limit neither the localization-electron model and nor the itinerant-electron model is applicable. It is observed from the resistivity curve that at low temperature as the V-V distance decreases the V^{3+}-3d electrons approaches to the Quantum Phase Transition (QPT) from the localized-electron side. Thermally activated behaviour of small polarons for all these vanadates is observed from temperature variation of thermoelectric data. From the variation of $d\chi/dT$ with T plot it is observed that with increase of Mn, that is, with the increase of chemical pressure structural transition is suppressed. Along with T_N, also the charge gap and activation energy of the vanadates depend on the V-V separation and as it decreases a breakdown of localized electron model for the 3d electrons is observed. The XPS study also indicates that with decreasing V-V separation the system moves towards the itinerant electron limit. Ti-doped ZnV_2O_4 samples show some un-usual behaviour. With Ti doping metal-metal distances increase but at the same time T_N increases. It deserves further study to explain the actual mechanism in these Ti doped samples.

References

[1]. Brinkman, W. F. and Rice, T. M., Application of Gutzwiller's Variational Method to the Metal-Insulator Transition, Phys. Rev. B, 2, 4302-4304, 1970.

[2]. Goodenuogh, J. B., Structure and Bonding, springer Verlag Berlin, Vol. 98 chapter 1 & 2, 2001.

[3]. Blanco-Canosa, S., Rivadulla, F., Pardo, V., Baldomir, D., Zhou, J. S., García-Hernández, M., López-Quintela, M. A., Rivas, J. and Goodenough, J. B., Enhanced Pressure Dependence of Magnetic Exchange in $A^{2+}[V_2]O_4$ Spinels Approaching the Itinerant Electron Limit, Phys. Rev. Lett., 99, 187201/1-187201/4, 2007.

[4]. Harrison, W. A., Editor, in Electronic structure and the properties of solid: The Physics of the chemical bond, Freeman, W. H. & co. San Francisco, 1980.

[5]. Bloch, D., The 10/3 law for the volume dependence of superechange, J. Phys. Chem. Solids. 27, 881-865, 1966.

[6]. Zhou, J. S. and Goodenough, J. B., Pressure-Induced Transition from Localized Electron Toward Band Antiferromagnetism in $LaMnO_3$, Phys. Rev. Lett. 89, 087201/1-087201/4, 2002.

[7]. Goodenough, J. B., Longo, J. M. and Kafalas, J. A., Band Antiferromagnetism and the New Perovskite $CaCrO_3$, Mater. Res. Bull. 3, 471-482, 1968.

[8]. Pardo, V., Blanco-Canosa, S., Rivadulla, F., Khomski, D. I., Bladomir, D., Wu, H. and Rivas, J., Homopolar Bond Formation in ZnV_2O_4 Close to a Metal-Insulator Transition, Phys. Rev. Lett., 101, 256403/1-256403/4, 2008.

[9]. Baldomir, D., Pardo, V., Blanco-Canosa, S., Rivadulla, F., Rivas, J., Piñeiro, A. and Arias, J. E., Pressure-induced metal–insulator transition in MgV_2O_4, Physica B, 403, 1639-1641, 2008.

[10]. Kuntscher, C., Rabia, K. , Forthaus, M. K. , Abd-Elmeguid, M. M. , Rivadulla, F., Kato, Y. and Batista, C. D., Nonmonotonic evolution of the charge gap in ZnV_2O_4 under pressure, Phys. Rev. B, 86, 020405/1-020405 /5(R), 2012.

[11]. Tsunetsugu, H. and Motome, Y., Magnetic transition and orbital degrees of freedom in vanadium spinels, Phys. Rev. B, 68, 060405/1-060405/4(R), 2003.

[12]. Y. Kato, Chern, G. W. , Al-Hassanieh, K. A., Perkins Natalia, B. and Batista, C. D., Orbital Disorder Induced by Charge Fluctuations in Vanadium Spinels, Phys. Rev. Lett. 108, 247215/1-247215/5, 2012.

[13]. Nizioł, S., Investigation of magnetic properties of ZnV_2O_4 spinel, Phys. Status Solidi A, 18, K11- K13, 1973.

[14]. Rechuis, M., Krimmel, A., N. Büttgen, Loidl, A. and Prokofiev, A., Crystallographic and magnetic structure of ZnV_2O_4: Structural phase transition due to spin driven Jahn Teller distortions, Eur. Phys. J. B, 35, 311-316, 2003.

[15]. Ueda, Y., Fujiwara, N. and Yasuoka H. , Magnetic and Structural Transitions in (Li$_x$Zn$_{1-x}$)V$_2$O$_4$ with the Spinel Structure, J. Phys. Soc. Jpn. 66, 778-783, 1997.

[16]. Blanco-Canosa, S., Rivadulla, F., Pardo, V., Baldomir, D., Zhou, J. S., García-Hernández, M., López-Quintela, M. A. , Rivas, J. and Goodenough, J. B., Enhanced Pressure Dependence of Magnetic Exchange in A^{2+} $[V_2]O_4$ Spinels Approaching the Itinerant Electron Limit, Phys. Rev. Lett., 99, 187201/1-187201/1, 2007.

[17]. Takubo, K., Son, J. Y., Mizokawa, T., Ueda, H., Isobe, M., Matsushita, Y. and Ueda, Y., Electronic structure of AV_2O_4 (A=Li, Zn, and Cd) studied by x-ray photoemission spectroscopy, Phys Rev. B, 74, 155103/1-155103/5, 2006.

[18]. Givonetti, G., Stroppa, A., Picozzi, S., Baldomir, D., Pardo, V., Blanco-Canosa, S., Rivadulla, F., Jodlauk, S., Niermann, D., Rohrkamp, J., Lorentz, T., Streltsov, S., Khomski, D. I. and Hemberger, J., Dielectric properties and magnetostriction of the collinear multiferroic spinel CdV_2O_4, Phys. Rev. B, 83, 060402/1-060402/4(R), 2011.

[19]. Goodenuogh, J. B., In proceedings of the climax "4th international conference on chemistry and uses of molybdenum", edited by Barry, H. F. and Mitchell, P. C. H., climax Molybdnum co., Ann Arbor, MI, P-1, 1982.

[20]. Goodenough, J. B., Metallic oxides, Solid. State. Chem., 5, 145–399,1971.

[21]. Luo, J., Liang, J. K., Liu, Q. L., Liu, F. S., Zhang, Y., Sun, B. J., Rao, G. H., Structure and magnetic properties of Mn-doped ZnO nanoparticles, J. Appl. Phys., 97, 086106/1-086106/3, 2005.

[22]. Kiswandhi, A., Brooks, J. S., Lu, J., Whalen, J., Siegrist, T. and Zhou, H. D., Chemical pressure effects on structural, magnetic, and transport properties of $Mn_{1-x}Co_xV_2O_4$, Phys. Rev. B, 84, 205138/1-205138/7, 2011.

[23]. Zhang, Z., Louca, Despina, Visinoiu, A., Lee, S.-H., Thompson, J. D., Proffen, T., Llobet, A., Qiu, Y., Park, S. and Ueda, Y., Local order and frustration in the geometrically frustrated spinels $Cd_{1-x}Zn_xV_2O_4$, Phys. Rev. B, 74, 014108/1-014108/9, 2006.

[24]. Kismarahardja, A., Brooks, J. S., Kiswandhi, A., Matsubayashi, K., Yamanaka, R., Uwatoko, Y., Whalen, J., Siegrist, T. and Zhou, H. D., CoV_2O_4: A Spinel Approaching the Itinerant electron Limit, Phys. Rev. Lett., 106, 056602/1-056602/4, 2011.

[25]. Schmidt, M., Ratcliff, W., Radaelli, P. G., Refson, K., Harrison, N. M. and Cheong, S.W., Spin Singlet Formation in $MgTi_2O_4$: Evidence of a Helical Dimerization Pattern Phys. Rev. Lett., 92, 056402/1-056402/4, 2004.

[26]. Sawatzky, A. and Post, D., X-ray photoelectron and Auger spectroscopy study of some vanadium oxides, Phys. Rev. B, 20, 1546-1551, 1979.

[27]. Maiti, K. and Sarma, D. D., Spectroscopic investigations of the electronic structure and metal-insulator transitions in a Mott-Hubbard system $La_{1-x}Ca_xVO_3$, Phys. Rev. B, 61, 2525-2534, 2000.

[28]. Konstantinović, M. J., Van den Berghe, S., Isobe, M. and Ueda, Y., X-ray photoelectron spectroscopy study of mixed-valence effects and charge fluctuation in $Na_xV_2O_5$, Phys. Rev. B, 72, 125124/1-125124/6, 2005.

[29]. Fujimori, A., Kawakami, K. and Tsuda, N., Electron correlation in low-carrier-density metals: photoemission study of the hole-doped Mott insulator $Li_xZn_{1-x}V_2O_4$, Phys. Rev. B, 38, 7889-7892(R), 1988.

[30]. Matsuno, J., Fujimori, A. and Mattheiss, L. F., Electronic structure of spinel type LiV_2O_4 Phys. Rev. B, 60, 1607-1610, 1999.

[31]. Matsuno, J., Kobayashi, K., Fujimori, A., Mattheiss, L. F and Ueda, Y., Electronic structure of the "heavy-fermion" systems LiV_2O_4, Physica B, 281-282, 28-29, 2000.

[32]. Harrison, W. A., Electronic Structure and the Properties of Solid, Dover, New York, 1989.

[33]. Tchernyshyov, O., Structural, Orbital, and Magnetic Order in Vanadium Spinels, Phys. Rev. Lett., 93, 157206/1-157206/4, 2004.

[34]. Khomskii, D. I. and Mizokawa, T., Orbitally Induced Peierls State in Spinels, Phys. Rev. Lett., 94, 156402/1-156402/4, 2005.

[35]. Isobe, M. and Ueda, Y., Observation of phase Transition from Metal to Spin-singlet Insulator in $MgTi_2O_4$ with S=1/2 Pyrochlore lattice, J. Phys. Soc. Jpn., 71, 1848-1851, 2002.